PHYSICAL REVIEW E VOLUME 49, NUMBER 3 MARCH 1994

# Experimental observation of transmission- and self-emission-type radiation transport in x-ray-produced plasmas

T. Endo,* H. Shiraga, H. Nishimura, A. Fujishima, K. Shigemori, Y. Kato, S. Nakai, and C. Yamanaka*

*Institute of Laser Engineering, Osaka University, 2-6 Yamada-oka, Suita, Osaka 565, Japan*

(Received 29 November 1993)

Radiation transport in x-ray-produced plasmas was experimentally studied. Thin foils of low-$Z$ and high-$Z$ materials were heated by external x rays from one side, and x rays emanating from the opposite side were observed. Careful measurements were made to distinguish between self-emitted x rays from the heated plasma and a transmitted component of the heating x rays. The results clearly demonstrate the existence of two types of radiation transport. The transmitted x rays play a major role in radiation transport in the case of a low-$Z$ material which is optically thin after burnthrough, and the self-emitted x rays play a major role in the case of a high-$Z$ material which is optically thick even after burnthrough.

PACS number(s): 52.25.Nr, 44.40.+a, 52.50.Jm

Due to the development of high-power lasers, it has become possible to use a laser-produced plasma as an intense x-ray source. Intense x-ray heating of solid targets enables uniform acceleration of the target and production of hot, dense plasmas in local thermodynamic equilibrium. Using these properties, plasma production by x-ray heating became a useful experimental technique in the research fields of laser fusion [1,2], hydrodynamic instability [3,4], equations of state [5], and atomic physics [6–11]. However, detailed properties of the x-ray-produced plasmas have not yet been well studied. Particularly, radiation transport is one of the most important issues.

In theoretical investigation, radiation transport in x-ray-produced plasmas is in general classified into two types: one for optically thick plasmas [12,13], and the other for optically thin plasmas [12,14]. In optically thick plasmas, radiative energy is transported mainly by self-emitted x rays from the heated plasma, which we call the self-emitted x rays hereafter. We call this type of radiation transport the self-emission type. On the other hand, in optically thin plasmas, radiative energy is transported mainly by the transmitted component of the heating x rays, which we call the transmitted x rays hereafter. We call this type of radiation transport the transmission type. For detailed investigation of the radiation transport, therefore, it is necessary to distinguish experimentally between the self-emitted and transmitted x rays. In previous experimental works on radiation transport in x-ray-produced plasmas, however, the results were analyzed without experimental distinction between these two components [15,16].

In this paper, we report a clear observation of these two types of radiation transport based on experimental distinction between the self-emitted and transmitted x-ray components. Thin foils of low-$Z$ and high-$Z$ materials were heated by laser-plasma x rays from one side and the x rays emanating from the other (rear) side were observed. The experimental arrangement was carefully designed to distinguish between the self-emitted and transmitted x rays. The experimental results clearly show that the radiation transport is the transmission type in the low-$Z$ plasma, while it is the self-emission type in the high-$Z$ plasma. Furthermore, observation of the temporal evolutions of the spectral transmittance clarifies the physical processes that take place in the two types of radiation transport. Therefore this is an experimental validation of the theoretical treatment of the two types of radiation transport described above.

The experimental arrangement is shown in Fig. 1. The x-ray source was a gold plate which was irradiated by one of the horizontal beams of frequency-tripled Gekko-XII Nd:glass laser [17] with an energy of 500 J at 351 nm. The laser beam irradiated the gold plate at an incidence angle of 40° from the normal with an elliptical spot whose minor axis was 0.4 mm. A thin foil of either a low-$Z$ or a high-$Z$ material was glued on the x-ray-irradiated side of an aperture plate, covering a 0.4-mm-diam diagnostic hole which defined the observed area of the thin foil. The low-$Z$ material was 0.90-$\mu$m-thick $CF_{1.317}$ (density: 1.99 g/cm$^3$) coated on a 0.21-$\mu$m-thick $C_8H_8$ (density: 1.12 g/cm$^3$), which we call a CF foil hereafter. The CF foil was heated by x rays from the $CF_{1.317}$ side. The high-$Z$ material was a 0.21-$\mu$m-thick Au foil. X rays emanating through the diagnostic hole were observed with a transmission-grating spectrometer coupled with an x-ray streak camera (TG-XSC) to which a time fiducial uv signal was supplied. Absolute spectral response of the photocathode of the TG-XSC was calibrated against an absolutely calibrated Kodak 101 x-ray film [18]. The temporal and spectral resolutions of the TG-XSC were approximately 130 ps and 10 Å, respectively. We used two types of targets: type $A$ and type $B$, which are shown in Figs. 1(a) and 1(b), respectively. In the case of the type-$A$ target, the x-ray source was viewed through the diagnostic hole, and both the transmitted and self-emitted x rays

*Permanent address: Institute for Laser Technology, 2-6 Yamada-oka, Suita, Osaka 565, Japan.

 

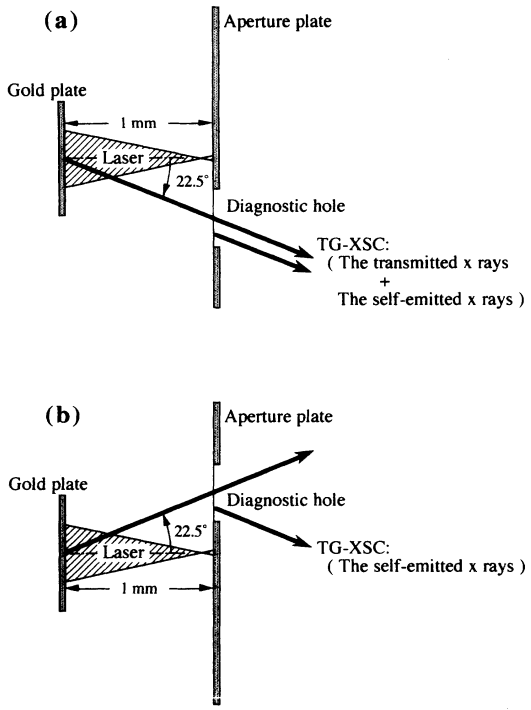


FIG. 1. Schematic side views of the experimental arrangement. (a) Type-*A* target. (b) Type-*B* target. TG-XSC denotes a transmission-grating spectrometer coupled with an x-ray streak camera.

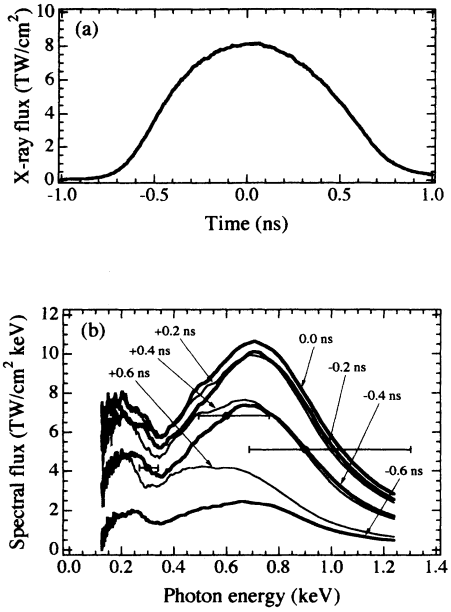


FIG. 2. Heating x rays on the thin foil. (a) Temporal profile of the heating x-ray flux, which was spectrally integrated from 10 to 95 Å. (b) Time-resolved spectra of the heating x rays. Horizontal error bars show typical spectral resolution.

were observed. In the case of the type-*B* target, the x-ray source was not viewed through the diagnostic hole, and only the self-emitted x rays were observed.

A preliminary experiment was made for characterization of the heating x rays. A gold plate not equipped with the aperture plate shown in Fig. 1 was irradiated with a laser beam in the same conditions as described above. In addition to the TG-XSC, two transmission-grating spectrometers coupled with Kodak 101 x-ray films (TG-F's) were used for diagnostics. Each TG-F was equipped with a pinhole grating resulting in a spatial resolution of approximately 50 $\mu$m in one dimension. One TG-F was placed at 22.5° from the target normal. More than 80% of the total x rays were emitted from within the laser spot on the target and there was no remarkable spatial structure in the soft-x-ray image. Another TG-F was placed tangential to the target in order to observe the x-ray emission from the blowoff expanding plasma. X-ray energy emitted to the tangential direction was less than 10% of that to the direction of 22.5° from the target normal. From these results, we can simply model the x-ray source as a uniform surface emitter with the size of the laser spot. The temporal evolution of the heating x rays on the thin foil was estimated from the measurement with the TG-XSC and geometrical calculation. Results of the estimation for the time dependence of the total flux and the spectral flux at different times are shown in Figs. 2(a) and 2(b), respectively; here the fluxes spatially averaged over the observed area of the thin foil are shown. The influence of the target structure on the source x rays (the x-ray flux on the thin foil) was estimated to be less than 1.3% by geometrical calculation where 100% diffusive (with cosine angular distribution) x-ray reemission of the target structure was assumed. Nonuniformity of the heating x-ray flux in the observed area of the thin foil was estimated to be ±26%. Accuracy of the photocathode calibration was ±13%. Reproducibility of the x-ray emission from the x-ray source was ±5.6%. As shown in Fig. 2(a), the heating x-ray flux at its peak time ($t=0.0$ ns) was $8\times10^{12}$ W/cm$^2$, which corresponds to the brightness temperature of 95 eV. However, it should be noted that the heating-x-ray spectrum at $t=0.0$ ns shown in Fig. 2(b) is significantly different from the Planckian spectrum of 95 eV. Also it should be noted that the thin foil is irradiated in this work by the heating x rays from a well-defined direction. This is in contrast with the case where a foil is placed at an opening of an x-ray-confining cavity [15] where the foil is heated by x rays from close to $2\pi$ directions.

The temporal profile of the observed x-ray intensity using a type-*A* target without a thin foil, which serves as a reference, is shown by the thin curves in Figs. 3(a) and 3(b). The observed x-ray intensities using the type-*A* and type-*B* targets are shown by the thick curves for the CF foil in Fig. 3(a) and for the Au foil in Fig. 3(b). The x-ray intensities in Figs. 3(a) and 3(b) are spectrally integrated (from 10 to 95 Å). We did the null test using a type-*B* target without a thin foil, in order to take account of expansion of the x-ray-source gold plasma. The error bars in Figs. 3(a) and 3(b) were determined on the basis of the null test.

Temporal profiles of the self-emitted x rays, which were observed using the type-*B* targets, show that foil burnthrough finished near $t=0.0$ ns for both the CF and Au foils. This means that rapid increase of the self-emitted x-ray intensity, which reflects mainly the rapid

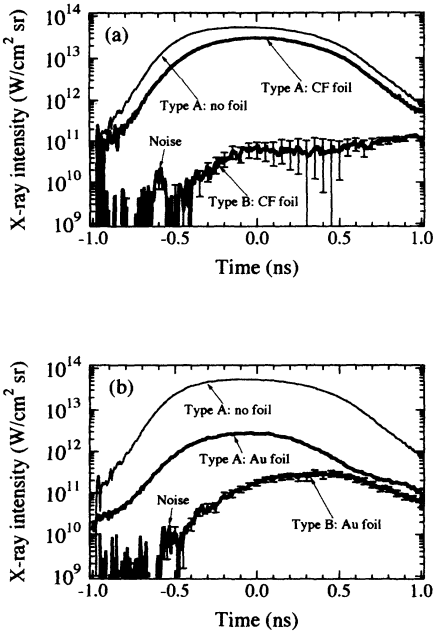


FIG. 3. Temporal profiles of the observed x-ray intensities. Humps labeled "Noise" are electrical noises of the x-ray streak camera. (a) Results for the CF foil. (b) Results for the Au foil.

rise in the temperature at the rear surface of the thin foil, finished near $t=0.0$ ns [19]. The areal density of the CF foil is 202.6 $\mu$g/cm$^2$, whereas the areal density of the Au foil is 405.7 $\mu$g/cm$^2$, which is twice as large as that of the CF foil. Therefore the burnthrough rate of the Au foil is almost twice as large as that of the CF foil, because the foil burnthrough occurs at almost the same time for both the CF and Au foils.

For discussion of the radiation transport, we have to consider not only intensities but also fluxes [20]. We denote the observed spectrally integrated intensities for the type-$A$ target without a foil, type-$A$ target with a foil, and type-$B$ target with a foil, as $I_0$, $I_A$, and $I_B$, respectively. The intensity of the self-emitted x rays $I_S$ is written by $I_S=I_B$. Due to symmetric arrangement of the diagnostic holes between the type-$A$ and type-$B$ targets, the intensity of the transmitted x rays $I_T$ is given by $I_T=I_A-I_B$. Since the directionality of the heating x rays is well defined, the flux of the transmitted x rays $S_T$ is given by $S_T=S_0(I_T/I_0)$, where $S_0$ is the heating x-ray flux, and $(I_T/I_0)$ is the transmittance of the heated foil to the heating x rays. The flux of the self-emitted x rays $S_S$ depends on the angular distribution of the self-emitted x rays, which we did not directly measure in this experiment. Assuming a uniform slab plasma in local thermodynamic equilibrium, the angular distribution of the self-emitted x rays is determined by the optical thickness of the plasma [20]. When the plasma is optically thick, the angular distribution becomes a cosine distribution and $S_S=\pi I_S$. On the other hand, when the plasma is optically thin, it becomes isotropic and $S_S=2\pi(\cos 22.5°)I_S$ (where 22.5° is the observation angle from the target normal). Figure 4 shows the temporal evolution of the flux ratio $S_T/(S_T+S_S)$, which is the ratio between the transmitted x-ray flux and the total x-ray flux, evaluated

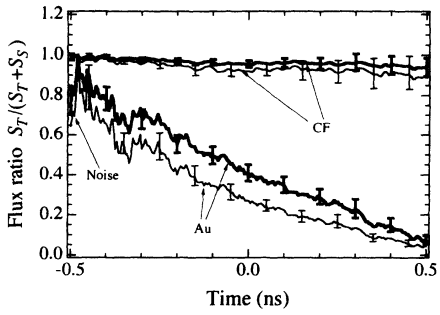


FIG. 4. Temporal evolution of the flux ratio $S_T/(S_T+S_S)$. Thick and thin curves correspond, respectively, to the evaluations based on cosine and isotropic angular distributions of the self-emitted x rays.

for the cosine and isotropic angular distributions of the self-emitted x rays. At the beginning of the x-ray heating where the thin foil is cold and can be regarded as a passive filter, the flux ratio should be essentially unity. As shown in Fig. 4, at an early stage of the x-ray heating, before $t=-0.4$ ns for example, the flux ratios are close to unity for both the CF and Au foils, implying that most of the thin foil remained rather cold. After the complete burnthrough, after $t=0.0$ ns for example [21], there is a remarkable difference between the CF and Au cases. In the case of the CF foil where the flux ratio is close to unity, the flux of the transmitted x rays is the main part of the total x-ray flux. On the other hand, in the case of the Au foil where the flux ratio is much smaller than unity, the flux of the self-emitted x rays is the main part of the total x-ray flux. After the complete burnthrough, the heated foil is a hot and expanded plasma, and therefore simulates a blowoff plasma in x-ray-driven plasma ablation. It is concluded from this observation that the types of the radiation transport in x-ray-produced low-$Z$ (CF) and high-$Z$ (Au) plasmas are the transmission type and the self-emission type, respectively.

Figure 5 shows the measured spectral transmittances of the heated foils, for which the self-emitted x rays have been subtracted. The spectral transmittances shown in Fig. 5 are those at $t=-0.4$ ns which corresponds to an early stage of the x-ray heating, and $t=+0.1$ ns which corresponds to a final stage of the burnthrough. Heating

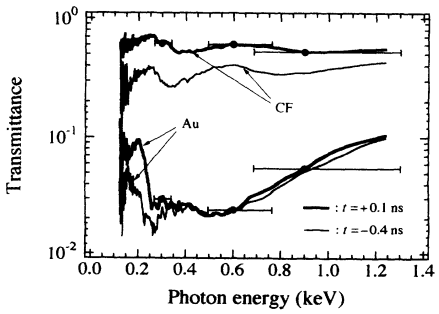


FIG. 5. Spectral transmittances of the heated foils measured at 22.5° from the target normal. Horizontal error bars show typical spectral resolution.

of the low-$Z$ (CF) plasma makes its transmittance increase drastically. That is, the x-ray-heated low-$Z$ plasma becomes quasitransparent to the external heating x rays. This is the direct experimental evidence for the ionization burnthrough [22], which is the essential feature for the transmission-type radiation transport. On the contrary, heating of the high-$Z$ (Au) plasma does not drastically change its transmittance. That is, the x-ray-heated high-$Z$ plasma remains opaque to the external heating x rays. Therefore the radiation transport in the x-ray-produced high-$Z$ plasma can be properly called the self-emission type.

In conclusion, we reported an unambiguous experimental observation of the two types of radiation transport in x-ray-produced plasmas. In the case of the low-$Z$ (CF) plasma, the radiation transport is the transmission type, whereas it is the self-emission type in the case of the high-$Z$ (Au) plasma. Spectral transmittances of the low-$Z$ and high-$Z$ plasmas have also been shown. Temporal evolution of the spectral transmittance of the low-$Z$ plasma clearly showed the ionization burnthrough, whereas that of the high-$Z$ plasma did not. This work was designed to clearly demonstrate the existence of the two types of radiation transport. However, the type of radiation transport is in general determined by the transparency of the plasma to the external heating x rays. In other words, the type of radiation transport depends not only on the material but also on the heating-x-ray conditions. Even with a low-$Z$ material, the radiation transport in the x-ray-produced plasma could become closer to the self-emission type for the cases of higher heating flux, longer pulse duration, and more oblique incidence angle.

We sincerely acknowledge contributions by the technical staffs at ILE for plasma diagnostics, target fabrication, and laser operation for this work.

[1] T. Mochizuki *et al.*, Jpn. J. Appl. Phys. **22**, L133 (1983).
[2] B. A. Hammel *et al.*, Phys. Rev. Lett. **70**, 1263 (1993).
[3] B. A. Remington *et al.*, Phys. Rev. Lett. **67**, 3259 (1991).
[4] G. Dimonte and B. Remington, Phys. Rev. Lett. **70**, 1806 (1993).
[5] R. Cauble *et al.*, Phys. Rev. Lett. **70**, 2102 (1993).
[6] S. J. Davidson *et al.*, Appl. Phys. Lett. **52**, 847 (1988).
[7] J. M. Foster *et al.*, Phys. Rev. Lett. **67**, 3255 (1991).
[8] T. S. Perry *et al.*, Phys. Rev. Lett. **67**, 3784 (1991).
[9] L. B. Da Silva *et al.*, Phys. Rev. Lett. **69**, 438 (1992).
[10] W. Schwanda and K. Eidmann, Phys. Rev. Lett. **69**, 3507 (1992).
[11] P. T. Springer *et al.*, Phys. Rev. Lett. **69**, 3735 (1992).
[12] K. Nozaki and K. Nishihara, J. Phys. Soc. Jpn. **48**, 993 (1980).
[13] R. Pakula and R. Sigel, Phys. Fluids **28**, 232 (1985); **29**, 1340(E) (1986).
[14] N. Kaiser, J. Meyer-ter-Vehn, and R. Sigel, Phys. Fluids B **1**, 1747 (1989).
[15] R. Sigel *et al.*, Phys. Rev. Lett. **65**, 587 (1990).
[16] T. Mochizuki *et al.*, Phys. Rev. A **36**, 3279 (1987).
[17] C. Yamanaka *et al.*, Nucl. Fusion **27**, 19 (1987).
[18] H. Nishimura *et al.*, J. X-ray Sci. Tech. **3**, 14 (1991).
[19] The gradual increase of the self-emission for the Au foil in the latter half of the x-ray heating, which peaks near $t = +0.4$ ns, is due to the additional heating by the collision of the plasma, which was blown off from the x-ray-source gold plate.
[20] Ya. B. Zel'dovich and Yu. P. Raizer, *Physics of Shock Waves and High-Temperature Hydrodynamic Phenomena* (Academic, New York, 1966), Chap. II.
[21] From another experiment using the same configuration as that described in this paper, it was found that influence of the collision of the plasma, which was blown off from the x-ray-source gold plate, was not negligible after $t = +0.25$ ns.
[22] D. Duston, R. W. Clark, J. Davis, and J. P. Apruzese, Phys. Rev. A **27**, 1441 (1983).

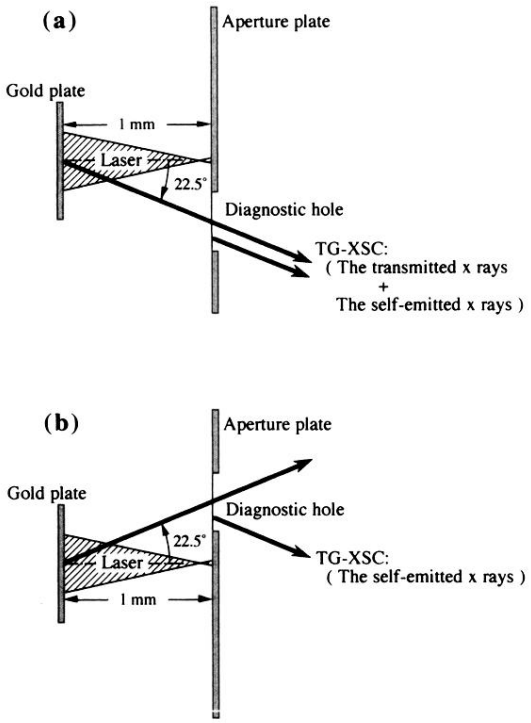


FIG. 1. Schematic side views of the experimental arrangement. (a) Type-*A* target. (b) Type-*B* target. TG-XSC denotes a transmission-grating spectrometer coupled with an x-ray streak camera.